Anomalous Refraction and Diffraction in Discrete Optical Systems

T. Pertsch,[1] T. Zentgraf,[2] U. Peschel,[1] A. Bräuer,[2] and F. Lederer[1]

[1]*Friedrich-Schiller-Universität Jena, Max-Wien-Platz 1, 07743 Jena, Germany*

[2]*Fraunhofer-Institut für Angewandte Optik und Feinmechanik, Schillerstrasse 1, 07745 Jena, Germany*

(Received 19 October 2001; published 12 February 2002)

We experimentally prove that light propagation in a discrete system, i.e., an array of coupled waveguides, exhibits striking anomalies. We show that refraction is restricted to a cone, irrespective of the initial tilt of the beam. Diffraction can be controlled in size and sign by the input conditions. Diffractive beam spreading can even be arrested and diverging light can be focused. The results can be thoroughly theoretically explained.

DOI: 10.1103/PhysRevLett.88.093901 PACS numbers: 42.25.Fx, 42.82.Et, 63.10.+a

Our understanding of light propagation primarily derives from isotropic media. The law of refraction predicts that the tilt of a beam traversing an interface between two media will monotonously grow with the angle of incidence. The law of diffraction predicts beam spreading being completely determined by the ratio of wavelength and width, only slightly affected by the refractive index and independent of the tilt. The reason for this behavior is the rotational symmetry of the isotropic medium. If this symmetry gets lost, as, e.g., in a stratified medium (Bragg mirror) or a discrete system (array of waveguides), these canonical laws of refraction and diffraction cease to hold. The mathematical background is the relation between the transverse (κ') and the longitudinal wave number component (β') of the wave vector, which constitutes the diffraction relation analog to the dispersion relation in the temporal domain. In two-dimensional isotropic media with a dielectric constant ε_r, we have $\beta' = 2\pi/\lambda\sqrt{\varepsilon_r - \kappa'^2}$, whereas in the general case this is a more complex function $\beta' = f(\kappa')$.

Here we will demonstrate anomalies in light refraction and diffraction in evanescently coupled waveguide arrays ("discrete" refraction and diffraction).

The first experiments on waveguide arrays date back to the early 1970's [1], when the first evidence of a discrete kind of diffraction was observed. But, only in the 1980's, Haus and co-workers revived the subject by showing some discrete imaging properties of waveguide arrays [2]. At the end of the 1980's, Christodoulides and Joseph predicted the existence of spatially solitary waves in nonlinear arrays [3] and initiated a great deal of theoretical work on discrete optical systems (for references, see [4]). This evolution culminated in the experimental evidence of discrete solitons in AlGaAs arrays in the late 1990's [5]. Although the peculiarities of discrete diffraction were identified as the origin of interesting nonlinear phenomena [6], such as beam defocusing in focusing Kerr media, and management of diffraction has been shown to be feasible [7], the very linear properties (discrete refraction and diffraction) have not been studied comprehensively yet. Recently the linear subject was reconsidered in demonstrating the appearance of photonic Bloch oscillations in waveguide arrays [8]. It is the aim of this Letter to draw a comprehensive picture of discrete diffraction and refraction in homogeneous waveguide arrays by confronting experimental and theoretical studies of this subject.

The experiments were performed on homogeneous arrays of 75 waveguides in an inorganic-organic polymer ($n_{co} = 1.554$) on thermally oxidized silicon wafers ($n_{sub} = 1.457$) with polymer cladding ($n_{cl} = 1.550$) (see Fig. 1). The 6 cm long samples were fabricated by uv lithography on 4 in. wafers. Each waveguide had a cross section of $3.5 \times 3.5\ \mu m^2$ and provided low loss single mode waveguiding (<0.5 dB/cm) at $\lambda = 633$ nm. The uniform separation of adjacent guides was $L = 8.5\ \mu m$ to achieve efficient evanescent coupling.

A HeNe laser beam was shaped with respect to width and tilt using a telescope and coupled into the array via the entrance facet with a microscope objective. The light emitted from the end facet is detected by a camera. Because light propagation along the array cannot be monitored, it is instead visualized by numerical simulations.

Obviously discreteness will matter if the input beam width compares to the period of the discrete system L. In Fig. 2 the most extreme case of a single channel excitation is displayed where the field shown represents the Green's function of the array [4,5], which differs from the continuous counterpart [6] considerably. On the other hand, intuition tells that for wide beams the continuous approximation should hold. Surprisingly, already an essentially four waveguide wide Gaussian input beam was found to retain its Gaussian shape upon propagation. To observe substantial diffractive spreading for a realistic propagation

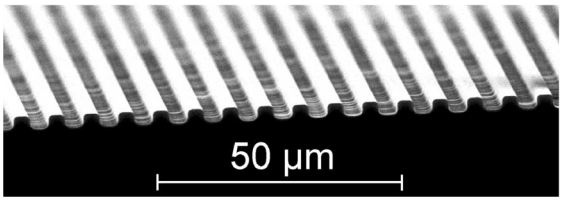

FIG. 1. Polymer waveguide array of 75 single mode waveguides (before applying the polymer cladding).

 © 2002 The American Physical Society

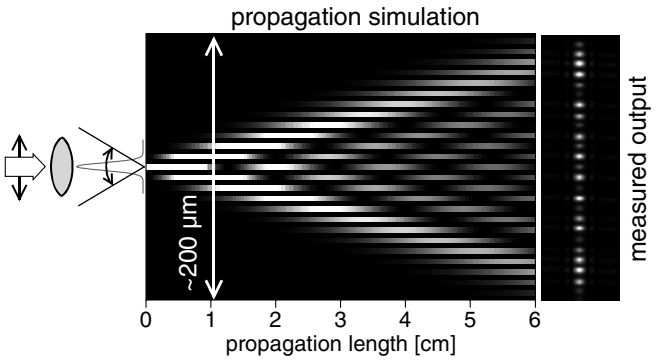

FIG. 2. A narrow input beam excites a single guide and produces a unique type of diffraction pattern, which is the Green's function of the array. Furthermore, discrete diffraction and refraction of wide tilted input beams is tested by off-axis illumination of the input objective.

length, we choose this width in all the experiments. In Fig. 3 the most spectacular consequences of anomalous refraction and diffraction are displayed. In Figs. 3(a) and 3(c) measurements and modeling show that, as in an isotropic medium, diffraction compares for two different input angles. But refraction is anomalous; i.e., the beam which is tilted 2.2° in front of the input facet exits the array at the same location as the untilted beam. On the contrary, Fig. 3(b) is an example for normal refraction but anomalous diffraction. The beam, which is tilted by 1.1°, crosses the array diffractionless.

To systematically study these anomalies, we varied the angle of incidence of the beam. This was achieved by shifting the laser beam off axis in front of the in-coupling microscope objective, resulting in a stationary focus on the input facet with a tilt proportional to the off-axis translation. We monitored the field at the output facet, the shift of which is proportional to the angle of propagation inside the array. For an isotropic system, this shift would monotonously grow with the tilt, and the beam width at the exit face would be invariant for changing tilt. In fact for small angles the transverse motion of the field in the array was found to be proportional to the initial tilt. But for growing angles this shift saturated and even reduced resulting in an oscillatory dependence (see Fig. 4). Evidently, two features of light propagation can be recognized; there is a maximum angle of propagation that cannot be exceeded and the width (strength of diffraction) varies with the input angle.

Interesting to note, the output field returns to the initial waveguide if a phase difference of integer multiples of π between adjacent waveguides is reached. For the corresponding initial beam tilt, the transverse motion of the field in the array is steadily prevented by Bragg reflection at the periodic array structure.

The theoretical analysis is based on a coupled mode theory, where the complete field evolution is reduced to that of the modal amplitudes a_n. The respective set of evolution equations reads as [2]

$$i\,\frac{d}{dz}\,a_n(z) + C[a_{n+1}(z) + a_{n-1}(z)] = 0\,, \qquad (1)$$

where a fast varying phase has been removed. Here z is the direction of propagation and C is a measure of the linear coupling between two waveguides amounting to $C = 109\ \mathrm{m}^{-1}$ for the polymer arrays used (see Fig. 1). The initial condition $a_n(z = 0)$ is determined by the overlap of the exciting beam $\vec{E}_{\mathrm{in}}(x, y)$ with the modal profile $\vec{E}_n(x, y)$ of the respective guide [9]. The whole incident field is mapped onto a finite number of mode amplitudes. Therefore phase differences between adjacent guides of multiples of 2π will have no effect on the field evolution. Apart from a reduced incoupling efficiency, the response of the array on initial tilts must be periodic as observed in the experiment.

A formal solution of Eq. (1) can be obtained as

$$a_n(z) = \int_{-\pi}^{\pi} d\kappa\, \tilde{a}(\kappa) \exp(i\kappa n) \exp[i\beta(\kappa)z], \qquad (2)$$

where κ is the transverse wave number multiplied with the waveguide spacing L. It is limited to the interval $(-\pi, \pi)$. The individual Fourier components $\tilde{a}$ are determined by the initial condition as

$$\tilde{a}(\kappa) = \frac{1}{2\pi} \sum_n a_n(z = 0) \exp(-i\kappa n)\,. \qquad (3)$$

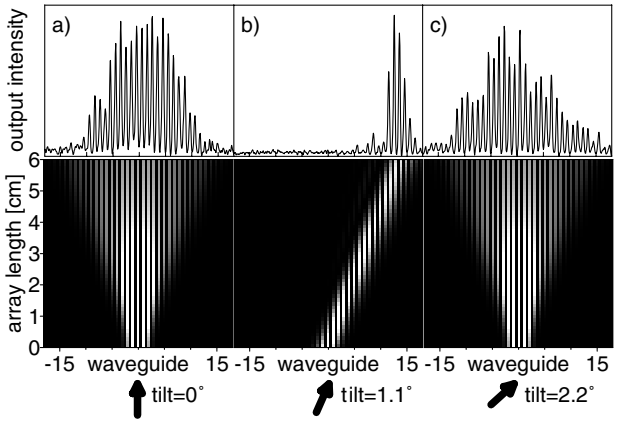

FIG. 3. Measured output intensity profile and simulated propagation for a Gaussian excitation with several input tilts.

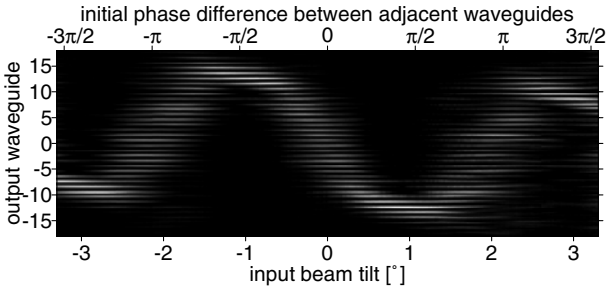

FIG. 4. Measured output intensity profiles vs tilt of a Gaussian input beam.

For a given initial condition, the field evolution is completely controlled by the diffraction relation $\beta(\kappa)$. It relates the longitudinal to the transverse wave number and determines how the individual Fourier components run out of phase during propagation. Following Eq. (1) this relation reads as

$$\beta(\kappa) = 2C\cos(\kappa), \tag{4}$$

being in strong contrast to the above discussed relation for isotropic media. In the case of the array, it is strictly periodic and can be regarded as a kind of band structure.

Because beams cover a few guides, the Fourier spectrum is finite with a central wave number κ_0, which is fixed by the tilt of the exciting beam. Hence, for convenience we can use a Taylor expansion of the diffraction relation (4) as

$$\beta(\kappa) \approx \beta(\kappa_0) + \gamma(\kappa - \kappa_0) + \frac{\delta}{2}(\kappa - \kappa_0)^2, \tag{5a}$$

$$\gamma = \left.\frac{d\beta}{d\kappa}\right|_{\kappa_0} = -2C\sin(\kappa_0), \tag{5b}$$

$$\delta = \left.\frac{d^2\beta}{d\kappa^2}\right|_{\kappa_0} = -2C\cos(\kappa_0). \tag{5c}$$

If we insert Eqs. (5) into the solution (2), we find that the evolution can be formally described by a partial differential equation:

$$\left[i\frac{\partial}{\partial z} + \beta(\kappa_0) - i\gamma\frac{\partial}{\partial n} - \frac{\delta}{2}\frac{\partial^2}{\partial n^2}\right]a'(n,z) = 0, \tag{6}$$

where n now appears as a continuous variable of the distributed amplitude function $a'(n,z) = a_n\exp(-i\kappa_0 n)$. Note that already Eq. (2) allows one to formally determine amplitudes for noninteger values of n and therefore to perform a continuous limit.

Applying the substitution $n' = n + \gamma z$, the first derivative in Eq. (6) disappears. This implies to term γ a transverse velocity. Moreover, Eqs. (5c) and (6) predict that the parameter δ determines the strength of diffraction; therefore we can call it diffraction coefficient. The dependence of these two quantities on the mean transverse wave number κ_0 reflects the anomalies in refraction and diffraction in an array. The most striking features are an upper limit of the velocity $\gamma_{\max} = -2C$ and diffractionless propagation ($\delta = 0$) at $\kappa_0 = \pi/2$. Evaluating the experimental results, we can prove these features quantitatively (see Fig. 5). In contrast to isotropic materials, diffractive spreading depends on the angle of incidence. Given a Gaussian beam where the amplitude in its focus is proportional to $\exp(-n^2/W_0^2)$ ($W_0 = 2$ in the experiments) and the focus is situated a distance p away from the entrance facet, the width W scaled to the waveguide spacing L will evolve similar to [10]

$$W(z) = W_0\sqrt{1 + \left(\frac{\lambda}{\pi W_0^2 L^2}p - \frac{2\delta}{W_0^2}z\right)^2}. \tag{7}$$

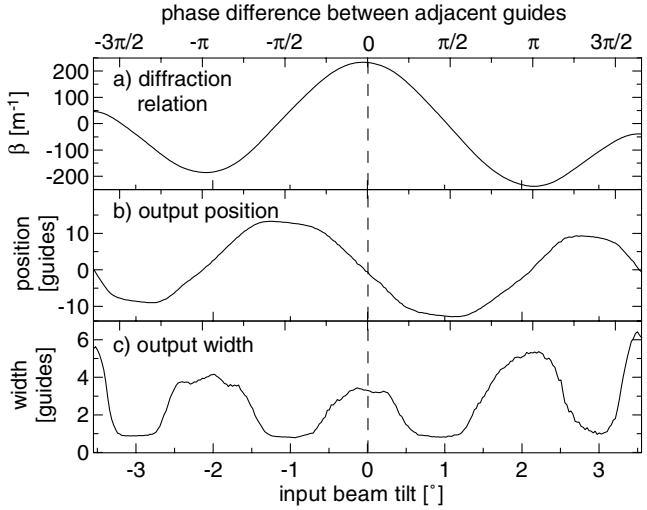

FIG. 5. Diffraction relation (a), output position (b), and output width (c) determined from the measurements in Fig. 4.

For the experiments reported above the focus was on the input facet ($p = 0$). In fact we find a good agreement between theoretical predictions [Eqs. (5c) and (7)] and experimental measurements [see Fig. 5(c)]. Note that, for a tilt of about 1.1°, corresponding to a phase difference of $\kappa = \pi/2$, the beam retains its original shape, i.e., diffraction is arrested as already observed in [8].

Interesting to note, the angle of diffractionless propagation is that of the maximum transverse velocity. It is the same angle under which the two intensity maxima of the single waveguide excitation disperse (see Fig. 2). Thus for diffractionless propagation the energy transport across the array is fastest.

The sign of the diffraction coefficient in Eq. (6) will change if the tilt of the exciting beam exceeds the angle of diffractionless propagation. But, according to Eq. (7) for $p = 0$, this has no effect on the width of the beam. This is reflected in the experiment by the similar output fields for an initial phase difference of 0 and π between adjacent guides [see Figs. 3(a) and 3(b)], where the slight differences are due to imperfections in the excitation with tilted beams. The situation is analogous to the identical dispersive spreading of an unchirped temporal pulse regardless if the medium exhibits a normal or an anomalous dispersion. Thus only experiments using beams with initial phase curvatures (chirp in the temporal case) can reveal a difference. This curvature will either be compensated or increased by diffraction, depending on the sign of the diffraction coefficient δ. The phase front curvature was realized by moving the focus either away from the input facet ($p > 0$) or into the sample ($p < 0$). In addition, the initial tilt was varied to change the diffraction coefficient δ.

Figure 6 shows the measured width of the output beam versus the input tilt for five different curvatures of the initial phase front. Figure 6(c) resembles the measurement of Fig. 5(c), where the focal plane coincides with the input

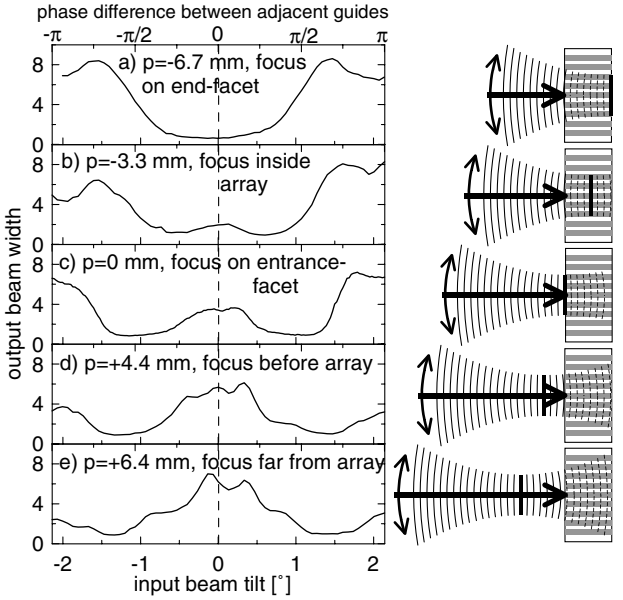

FIG. 6. Measured width of the output intensity profile vs input beam tilt for different positions of the focal plane of a Gaussian excitation.

facet giving a flat input phase. For Fig. 6(a) the focal plane coincides with the output facet ($p = -6.7$ mm). Thus "conventional diffraction" ($\delta < 0$), which is found for normal incidence, just leads to a maximal focusing of the input beam by compensating the initial phase front curvature. Tilting the beam and, consequently, decreasing and eventually changing the sign of diffraction results in an increased width of the output field. If the focal plane is in the middle of the sample [see Fig. 6(b)], the initial curvature is overcompensated for zero tilt. But slightly tilting the beam and therefore reducing the diffraction coefficient to half of its maximum value minimizes the output width. A further tilt results again in an increased width of the output beam. Moving the focal plane into the opposite direction, i.e., away from the sample, shows a reversed behavior. In Fig. 6(e) the objective is moved about as much away from the sample ($p = 6.4$ mm) as it was moved towards the sample in Fig. 6(a) compared to the situation in Fig. 6(c). Therefore the input beam has the same radius of curvature at the input facet, but with opposite sign. As a result, the curvature is enhanced at zero tilt and compensated for a phase difference of $\pm\pi$ between adjacent guides. A comparison of Figs. 6(a) and 6(e) clearly reveals the influence of the sign of the diffraction coefficient δ on beam spreading. While in Fig. 6(a) the minimum output width is achieved for $\delta(\kappa_0 = 0) = -2C$, it is accomplished for $\delta(\kappa_0 = \pm\pi) = 2C$ in Fig. 6(e). For a beam with a tilt of $\kappa_0 = \pm\pi$, diffractive spreading in air behind the beam waist is canceled in the array by a diffraction of opposite sign. Consequently, the beam waist is imaged onto the output facet. Therefore, a tilted array can be used as a simple imaging element.

In conclusion, we have studied the propagation of beams in homogeneous waveguide arrays. It turned out that refraction and diffraction exhibit strong anomalies as they depend periodically on the initial beam tilt. In contrast to isotropic systems, we found that the transverse energy transport cannot exceed a certain maximum velocity and that diffractive spreading depends on the direction of propagation; i.e., by varying the angle of incidence size and sign of diffraction can be controlled and it can even be arrested. Both effects are signatures of the diffraction relation of the array, which has been visualized experimentally. For particular initial tilts, the array can undo beam spreading (and phase curvature) accumulated upon propagation in an isotropic medium. Therefore, a tilted waveguide array can form a simple imaging system.

The authors gratefully acknowledge a grant of the Deutsche Forschungsgemeinschaft (SFB 196) and support by the European Community (IST-2000-26005).

[1] S. Somekh, E. Garmire, A. Yariv, H. Garvin, and R. Hunsperger, Appl. Phys. Lett. **22**, 46 (1973).
[2] H. Haus and L. Molter-Orr, IEEE J. Quantum Electron. **19**, 840 (1983).
[3] D. N. Christodoulides and R. I. Joseph, Opt. Lett. **13**, 794 (1988).
[4] F. Lederer, S. Darmanyan, and A. Kobyakov, in *Spatial Solitons,* edited by S. Trillo and W. Torruellas, Springer Series in Optical Sciences Vol. 82 (Springer, New York, 2001).
[5] H. S. Eisenberg, Y. Silberberg, R. Morandotti, A. Boyd, and J. S. Aitchison, Phys. Rev. Lett. **81**, 3383 (1998).
[6] R. Morandotti, H. S. Eisenberg, Y. Silberberg, M. Sorel, and J. S. Aitchison, Phys. Rev. Lett. **86**, 3296 (2001).
[7] H. S. Eisenberg, Y. Silberberg, R. Morandotti, and J. S. Aitchison, Phys. Rev. Lett. **85**, 1863 (2000).
[8] T. Pertsch, P. Dannberg, W. Elflein, A. Bräuer, and F. Lederer, Phys. Rev. Lett. **83**, 4752 (1999); R. Morandotti, U. Peschel, J. S. Aitchison, H. S. Eisenberg, and Y. Silberberg, Phys. Rev. Lett. **83**, 4756 (1999).
[9] *Guided-Wave Optoelectronics,* edited by T. Tamir (Springer-Verlag, Berlin, 1988).
[10] M. Born and E. Wolf, *Principles of Optics* (Pergamon Press, Oxford, 1985), 6th ed.